

Spin waves cause non-linear friction

M. P. MAGIERA¹ (a), L. BRENDEL¹, D. E. WOLF¹ and U. NOWAK²

¹ Faculty of Physics and CeNIDE, University of Duisburg-Essen, D-47048 Duisburg, Germany, EU

² Department of Physics, University of Konstanz, D-78457 Konstanz, Germany, EU

PACS 75.10.Hk – Classical spin models

PACS 68.35.Af – Atomic scale friction

PACS 75.30.Ds – Spin waves

Abstract. - Energy dissipation is studied for a hard magnetic tip that scans a soft magnetic substrate. The dynamics of the atomic moments are simulated by solving the Landau-Lifshitz-Gilbert (LLG) equation numerically. The local energy currents are analysed for the case of a Heisenberg spin chain taken as substrate. This leads to an explanation for the velocity dependence of the friction force: The non-linear contribution for high velocities can be attributed to a spin wave front pushed by the tip along the substrate.

Introduction. – On the macroscopic scale the phenomenology of friction is well-known. However, investigations of energy dissipation on the micron and nanometer scale have led in recent years to many new insights [1]. This progress was made possible by the development of modern surface science methods, in particular Atomic Force Microscopy, which allows to measure energy dissipation caused by relative motion of a tip with respect to a substrate.

Studies concerning the contribution of magnetic degrees of freedom to energy dissipation [2, 3] form a young subfield of nanotribology, which has been attracting increasing interest in recent years. Two classes of models have been considered, which show different phenomena. The first one is Ising-like spin systems with two equivalent half spaces moving relative to each other [4–8]. In this case, friction is induced by thermal fluctuations, and hence is not present at zero temperature. In the second class of models [9–13], there is no symmetry between slider and substrate: The slider, representing *e.g.* the tip of a Magnetic Force Microscope, interacts only locally with a planar magnetic surface. While scanning the surface, the tip in general excites substrate spins and hence experiences friction, even at zero temperature. The present study belongs to the second class of models.

We investigate the nature of the substrate excitations caused by the tip motion for a classical Heisenberg model with Landau-Lifshitz-Gilbert (LLG, [14, 15]) dynamics (precession around, and relaxation into the local field di-

rection). As the spins are continuous variables, spin wave excitations are possible. As we will show in the following, their properties are reflected in the velocity dependence of the friction force. Spin waves are increasingly attracting interest: *e.g.* in the last years a new subfield of magnetism, *magnonics*, has been developed, where materials are studied with respect to their spin wave properties [16, 17]. One motivation is to create new devices using spin wave logics or novel concepts of data storage.

In a previous work we showed that friction in this model is proportional to the scanning velocity v (“viscous behaviour”), provided that the tip does not move too fast [10]. The reason can be found in continuous excitations, while the motion in the Ising-model consists of discrete excitations and relaxations, which yields a constant friction force for low v . In the present paper we focus on the local dissipation processes in order to explain, why for high velocities deviations from the viscous behaviour exist.

Simulation model. – To simulate a solid magnetic material, we consider a chain of $N=320$ classical, normalised dipole moments (“spins”, *cf.* fig. 1) $\mathbf{S}_i = \boldsymbol{\mu}_i / \mu_s$, where μ_s denotes the material-dependent atomic magnetic moment. The spins represent magnetic moments of single atoms, arranged with a lattice constant a along the x -axis. Two lattice constants above the spin chain, a magnetic tip \mathbf{S}_{tip} moves with constant velocity $\mathbf{v} = v\mathbf{e}_x$. Its magnetisation is fixed in z -direction. At the beginning of each simulation the tip is positioned at the centre of the chain.

In order to keep boundary effects small, we use a conveyor belt technique with anti-periodic boundary condi-

(a)E-mail: martin.magiera@uni-due.de

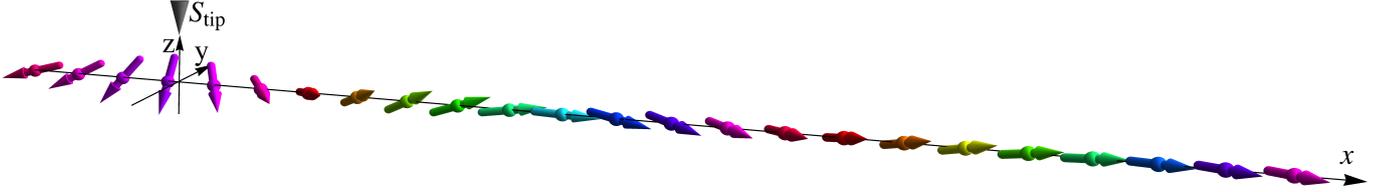


Fig. 1: Snapshot of a simulation. The colour encoding denotes the spins' orientation in the yz -plane (the tip is moved along the spin chain axis to the right). In front of the tip a spin wave is visible, *i.e.* an oscillation of the spins around the x -axis.

tions: When the tip has moved by one lattice constant, the boundary spin at the back end is deleted and a new spin with opposite direction is added at the front end of the chain. This shift puts the tip back to the centre of the simulation cell.

This paper analyses, how local excitations contribute to magnetic friction. Each substrate spin contributes its exchange interaction, $\mathcal{H}_{\text{sub}}^{(i)}$, and its interaction with the tip field, $\mathcal{H}_{\text{tip}}^{(i)}$ to the Hamiltonian

$$\mathcal{H} = \sum_{i=1}^N \left(\mathcal{H}_{\text{sub}}^{(i)} + \mathcal{H}_{\text{tip}}^{(i)} \right) = \sum_{i=1}^N \mathcal{H}^{(i)}. \quad (1)$$

As the substrate spins represent a ferromagnetic solid, we use the anisotropic Heisenberg-Hamiltonian,

$$\mathcal{H}_{\text{sub}}^{(i)} = -\frac{J}{2} \mathbf{S}_i \cdot (\mathbf{S}_{i+1} + \mathbf{S}_{i-1}) - d_z S_{i,z}^2. \quad (2)$$

$J > 0$ describes the ferromagnetic exchange interaction between \mathbf{S}_i and its nearest neighbours $i \pm 1$. In order to avoid double counting, half of the pair interaction is attributed to either spin. $d_z = -0.1J$ is the anisotropy constant: Here it defines an easy plane anisotropy, thus the substrate spins prefer an alignment in the xy -plane. The moving tip interacts with each substrate spin by the dipolar interaction,

$$\mathcal{H}_{\text{tip}}^{(i)} = -w \frac{3(\mathbf{S}_i \cdot \mathbf{e}_i)(\mathbf{S}_{\text{tip}} \cdot \mathbf{e}_i) - \mathbf{S}_i \cdot \mathbf{S}_{\text{tip}}}{R_i^3}, \quad (3)$$

where $R_i = |\mathbf{R}_i|$ is the length of the distance vector $\mathbf{R}_i = \mathbf{r}_i - \mathbf{r}_{\text{tip}}$, and \mathbf{e}_i its unit vector $\mathbf{e}_i = \mathbf{R}_i/R_i$. \mathbf{r}_i and \mathbf{r}_{tip} denote the position vectors of the substrate spins and the tip, respectively. w quantifies the dipole-dipole coupling of the substrate and the tip, with $w |\mathbf{S}_{\text{tip}}| = 10J a^3$ in this paper.

While the tip magnetisation direction is fixed in time, the substrate spins are allowed to change their orientation. To simulate their dynamics, we solve the LLG equation,

$$\dot{\mathbf{S}}_i = -\tilde{\gamma} [\mathbf{S}_i \times \mathbf{h}_i + \alpha \mathbf{S}_i \times (\mathbf{S}_i \times \mathbf{h}_i)], \quad (4)$$

numerically via the Heun integration scheme, where $\tilde{\gamma} = \gamma [\mu_s(1 + \alpha^2)]^{-1}$ with the gyromagnetic ratio γ . The first term represents the Larmor precession of each spin in the effective field,

$$\mathbf{h}_i = -\frac{\partial \mathcal{H}}{\partial \mathbf{S}_i} \quad (5)$$

with the precession frequency $\tilde{\gamma} |\mathbf{h}_i|$. The precessional motion preserves energy. Dissipation is introduced by the second term which causes an alignment towards \mathbf{h}_i . α is a material constant which can be obtained from ferromagnetic resonance experiments and represents the coupling of each spin to a reservoir of zero temperature. By adding a stochastic term to the effective field, it is possible to study the influence of finite temperatures as done in [10, 11]. However, in order to analyse the non-equilibrium excitations it is advantageous to suppress thermal spin waves by setting temperature equal to zero in this work.

In order to discuss frictional losses occurring in the system the *global* energy balance was analysed in [10]:

$$\frac{d\mathcal{H}}{dt} = P_{\text{pump}} - P_{\text{diss}}, \quad (6)$$

$$P_{\text{pump}} = \sum_{i=1}^N P_{\text{pump}}^{(i)} = \sum_{i=1}^N \frac{\partial \mathcal{H}_{\text{tip}}^{(i)}}{\partial \mathbf{r}_{\text{tip}}} \cdot \dot{\mathbf{r}}_{\text{tip}}, \quad (7)$$

$$P_{\text{diss}} = \sum_{i=1}^N P_{\text{diss}}^{(i)} = \sum_{i=1}^N \tilde{\gamma} \alpha (\mathbf{S}_i \times \mathbf{h}_i)^2. \quad (8)$$

The only explicit time-dependence of the Hamiltonian \mathcal{H} stems from the motion of the tip. It leads to the first term in eq. (6), which is the energy pumped into the spin system per unit time by an outside energy source that keeps the tip moving. Accordingly we call it the ‘‘pumping power’’. Its local contribution, $P_{\text{pump}}^{(i)}$, is the energy transferred per unit time from the tip to substrate spin \mathbf{S}_i . The friction force, $\mathbf{F} = -F \mathbf{e}_x$, the substrate exerts on the tip is given by

$$F = \frac{\langle P_{\text{pump}} \rangle}{v}, \quad (9)$$

where the angular brackets denote a time average over at least one period a/v .

$P_{\text{diss}}^{(i)}$ represents the energy current from spin \mathbf{S}_i into the heat bath. In other words, this is the energy dissipated at site i per unit time. Dissipation always occurs when the system relaxes towards the ground-state, in which the spin at site i is aligned with the local field-direction \mathbf{h}_i . Without tip movement, P_{pump} is zero and P_{diss} leads the system quickly to its ground state. For a tip moving at constant velocity, a steady non-equilibrium state is reached, where the time averaged derivative $\langle d\mathcal{H}/dt \rangle$ vanishes, because all energy pumped into the system is dissipated. Then the two power terms in eq. (6) cancel.

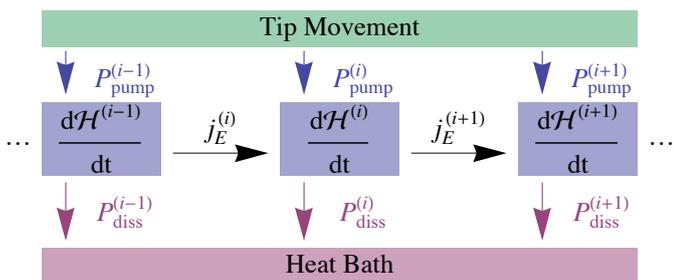


Fig. 2: Illustration of the local energy balance. The arrows represent the directions in which the energy transfers are counted positive: a positive $j_E^{(i)}$ rises the energy at site (i) , but lowers the one at site $(i-1)$.

When evaluating the *local* energy balance instead of eq. (6), energy currents j_E within the substrate have to be taken into account, which transport energy from one spin to its neighbour (cf. fig. 2). By taking the time derivative of the local Hamiltonian one obtains:

$$\frac{d\mathcal{H}^{(i)}}{dt} = P_{\text{pump}}^{(i)} - a (\text{div } j_E)^{(i)} - P_{\text{diss}}^{(i)}, \quad (10)$$

$$\begin{aligned} j_E^{(i)} &= -J(\mathbf{S}_i - \mathbf{S}_{i-1}) \cdot \frac{\dot{\mathbf{S}}_{i-1} + \dot{\mathbf{S}}_i}{2} \\ &= -\frac{J}{2}(\mathbf{S}_i \cdot \dot{\mathbf{S}}_{i-1} - \mathbf{S}_{i-1} \cdot \dot{\mathbf{S}}_i). \end{aligned} \quad (11)$$

Simulation Results. – Let us consider the steady state in a co-moving frame: the local quantities do not depend on spin index i and time t separately, but only on the (continuous) coordinate $x_i = \mathbf{R}_i(t) \cdot \mathbf{e}_x$. For considerations, where all spins are equivalent, we can drop the index i , *e.g.* the tip position is always at $x = 0$. In its vicinity, fig. 3(a) shows the local pumping power, as well as the discrete divergence of the energy current, $(\text{div } j_E)^{(i)} = (j_E^{(i+1)} - j_E^{(i)})/a$, as functions of x .

The physical interpretation of fig. 3(a) is the following: When the tip approaches, a substrate spin lowers its energy by adjusting to the inhomogeneous tip field at the cost of the exchange interaction. When the tip has passed by, it returns asymptotically to its higher energy in the absence of the tip field. This means that the tip injects energy $P_{\text{pump}}(x) \propto v$ per unit time at $x < 0$ and extracts apparently the same amount of energy from the substrate spins at $x > 0$. With respect to origin and curve shape, this is very similar to an electrical charge passing by a charge of opposite sign on a straight line. The apparent central symmetry holds only up to first order in v , though. The small asymmetry, not noticeable in fig. 3(a), is due to dissipation, which will be discussed below. But first we derive the steady state current within the chain.

In the steady state, we have

$$\dot{\mathbf{S}}_i = \dot{\mathbf{S}}(x_i) = v \partial_x \mathbf{S}(x_i) = v \frac{\mathbf{S}_{i+1} - \mathbf{S}_i}{a}, \quad (12)$$

where the third equality, due to using the difference quo-

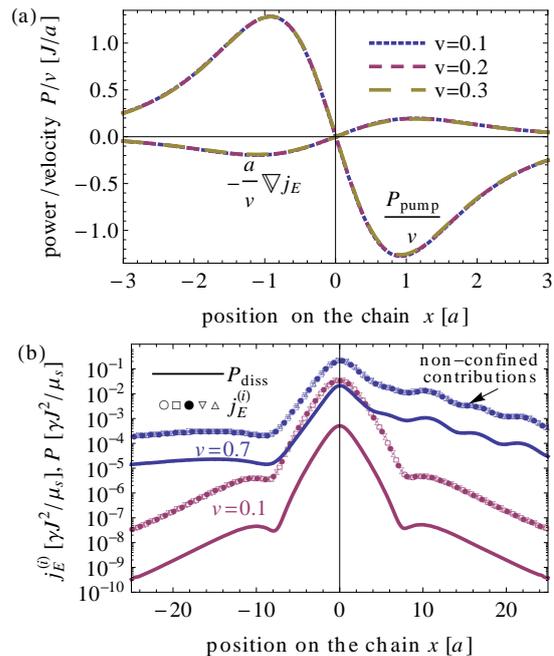


Fig. 3: (a) Pumping power and transported power, rescaled by velocity, at $\alpha = 0.1$. Negative pumping power represents an energy return from the spin chain to the tip, positive an energy injection from the tip into the chain. (b) Energy current for five different time steps (points, for $\alpha = 0.1$), as well as the dissipation power (solid lines). They turn out to be exactly proportional to each other, the coefficient being linear in αv .

tient, holds up to first order in a . Plugging that into eq. (11), the current $j_E^{(i)}$ reads

$$j_E^{(i)} = \frac{Jv}{2a}(1 - \mathbf{S}_{i-1} \cdot \mathbf{S}_{i+1}). \quad (13)$$

This shows that j_E transports the exchange energy to be paid for orienting the spins according to the inhomogeneous tip field. Correspondingly, the source of this current ($\text{div } j_E > 0$) is behind, and its sink ($\text{div } j_E < 0$) is in front of the tip, as seen in fig. 3(a).

The terms discussed so far are reversible and hence independent of the damping constant α : To first order in v they add up to zero in eq. (6). The origin of dissipation is that the spin pattern does not follow the tip instantaneously, but with a delay, which corresponds in the co-moving frame to a lag $\Delta x \propto \alpha v$ [10]. It is a manifestation of the *driving* out of equilibrium, which the spin relaxation must counteract. Fig. 3(b) shows that $P_{\text{diss}}(x)/j_E(x)$ is indeed a constant $\propto \alpha v$, which we may call the *driving force*¹. As pointed out in fig. 3(a), j_E is proportional to v . This only holds true for velocities not much larger than $v_0 \approx 0.31\gamma Ja/\mu_s$ (see eq. (16) below). This implies that for small velocities $P_{\text{diss}} \propto \alpha v^2$, which gives rise to a friction force, eq. (9), proportional to αv .

¹This is analogous to electrical power $P = UI$, where the voltage U provides the driving force for the current I .

Fig. 3(b) shows an important qualitative difference between energy currents for tip velocities below, respectively above v_0 . For low velocities, the energy current is concentrated around the tip position in an essentially symmetric way: Whatever exchange energy is released behind the tip, is reabsorbed in front of it. For high velocities, however, an additional shoulder in front of the tip appears. This shoulder represents a part of the energy current, which can leave the tip's immediate neighbourhood and propagates further along the spin chain, until it is damped out. We call this contribution *non-confined*. The propagation range depends on the damping constant α , as can be seen in fig. 4. The lower the damping constant, the farther the current extends.

In order to evaluate this quantitatively, we define the non-confined energy current as

$$j_{nc}(x) = j_E(x) - j_E(-x) \quad \text{for } x > 0. \quad (14)$$

It is plotted for several α -values in fig. 4(b). The axes are rescaled in order to show that the range shrinks with increasing damping approximately like $\alpha^{-0.4}$, and that the amplitude of the non-confined current also decreases roughly like $\alpha^{-0.4}$. The range and the amplitude of the non-confined current combine in such a way, that the integral over $j_{nc}(x)$ is nearly proportional to α^{-1} . Hence, when multiplied by the driving force $\propto \alpha v$, the α -dependence nearly cancels. The contribution of the non-confined excitations to friction is therefore approximately independent of α , in contrast to the confined contribution discussed above. As will be explained below, the two contributions also depend differently on velocity.

The non-confined excitations can be regarded as spin waves. An excitation means a deflection of a spin \mathbf{S}_i from the local field \mathbf{h}_i , leading to dissipation at the corresponding site according to eq. (8) and a precession around \mathbf{h}_i in a plane perpendicular to \mathbf{h}_i . Accordingly,

$$\mathbf{e}_{i,a} = \frac{\mathbf{h}_i \times \mathbf{e}_y}{|\mathbf{h}_i \times \mathbf{e}_y|} \quad \text{and} \quad \mathbf{e}_{i,b} = \frac{\mathbf{h}_i \times \mathbf{e}_{i,a}}{|\mathbf{h}_i \times \mathbf{e}_{i,a}|} \quad (15)$$

form an appropriate local basis to illustrate the excitations. Spins far in front of the tip experience a field which points in x -direction, thus the $\mathbf{e}_{i,a}$ -component points in z -direction. Near the tip the basis changes as sketched in the inset of fig. 5.

In the low velocity regime, a deflection from the local fields is present solely in the vicinity of the tip, according to the purely confined contribution to friction discussed above. For velocities, where non-confined currents can be observed, additional oscillations are present in front of the tip. A Fourier analysis of our simulation data shows that their wavenumber has approximately a linear velocity dependence:

$$k \propto v - v_0 \quad \text{with} \quad v_0 \approx 0.31 \gamma J a / \mu_s. \quad (16)$$

The resulting empirical coefficient 0.31 must be expected to depend on system parameters like the tip field's shape

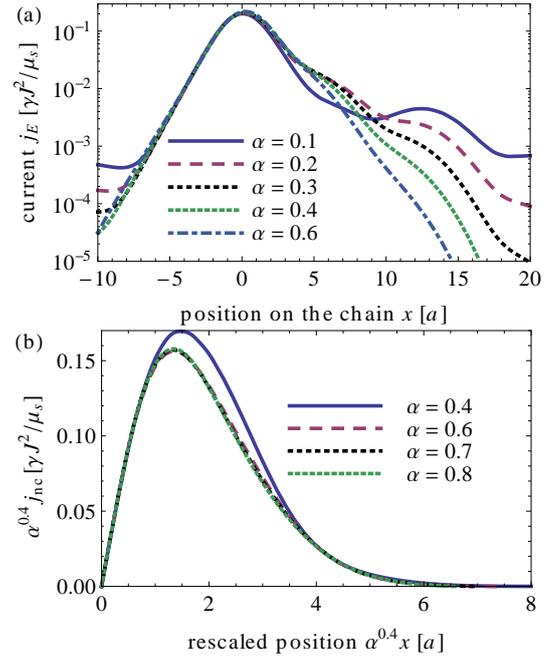


Fig. 4: (a) Energy currents for $v=0.6$ and some α values. When the damping is lowered, the current can proceed further in the substrate. (b) Rescaled non-confined current vs. a rescaled position for $v=0.85$.

and amplitude, which determine the spin waves' confinement. For small enough damping, the oscillations presumably extend arbitrarily far in front of the tip. Asymptotically we can neglect the tip field and consider an isolated spin chain with exchange interaction only. In its ground state, all spins point into the same direction, say \mathbf{e}_x . For small perturbations of \mathbf{S}_i from this direction, the LLG-equation with

$$\mathbf{h}_i = J(\mathbf{S}_{i-1} + \mathbf{S}_{i+1}) \quad (17)$$

can be linearised (*e.g.* [18]). The solution is a spin wave with an oscillating part of

$$\boldsymbol{\delta}_i = \mathbf{e}_y \delta \cos(ika - \omega t) + \mathbf{e}_z \delta \sin(ika - \omega t) \quad (18)$$

to first order in its small amplitude δ . Its dispersion relation

$$\omega(k) = 4 \frac{J\gamma}{\mu_s} (1 - \cos(ka)) \quad (19)$$

yields a group velocity $v \propto k$ in the long wavelength limit. The finding eq. (16) indicates that this holds true even in the more complicated system with the inhomogeneous tip field.

Inserting $\mathbf{S}_i = \mathbf{e}_x + \boldsymbol{\delta}_i$ into eqs. (17) and (8) yields for the wave of wave number k a dissipation of

$$P_{\text{diss}}(k) \propto \sin^4 \left(\frac{ka}{2} \right). \quad (20)$$

Using eq. (16) and assuming that the amplitude of the spin wave excitations δ does not depend on v and that $ka \ll 1$,

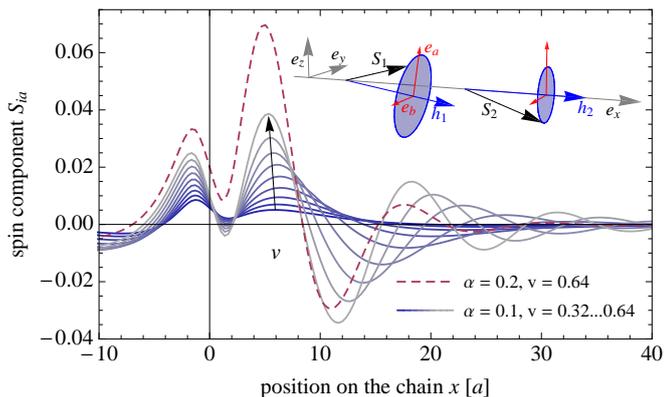


Fig. 5: Spin component perpendicular to the corresponding field. While for low velocities one precession around the local field is observable, for higher velocities more precession cycles in front of the tip are present. For lower damping excitations reach further. Sketch: Definition of the field dependent basis. For two sites spin and field values are sketched. For S_2 the local field points in x -direction (as the situation in the studied system in front of the tip is), and the spin precesses on the blue disk. The shift of the field for S_1 to the bottom (as it may be induced by the tip-field) yields also a change of the disk and the appropriate basis.

this predicts a non-linear velocity dependence of the spin wave contribution to friction like $\frac{(v-v_0)^4}{v}$.

The total magnetic friction force is thus predicted to be

$$F \approx A\alpha v + B(\alpha)\Theta(v - v_0)\frac{(v - v_0)^4}{v}, \quad (21)$$

where $\Theta(x)$ is the Heaviside step function, and the coefficients A , B as well as v_0 may depend on system parameters like the tip field. In fig. 6 this total force is plotted, and the simulation results are in good agreement with eq. (21).

Conclusion and outlook. – In this work, we could separate two distinct contributions to magnetic friction by examining the energy current in a spin chain. The confined current results in a friction force $F=A\alpha v$, which is in accord with our earlier results for $2d$ [10] and $3d$ [12] substrates. Above a threshold velocity v_0 , spin wave excitations may leave the tip's immediate neighbourhood and form a damped wave packet in front of the tip, propagating along with it. These excitations are the stronger, the weaker the damping. They lead to an additional contribution to friction with a non-linear velocity dependence. The dependence of the non-confined contribution on α is not trivial, because the range as well as the amplitude of the energy current are influenced in a non-linear way., cf. fig 4(b).

Important extensions of the present investigation include the influence of dimensionality on the non-confined spin waves. Here the propagation is not confined to the tip's motion direction. The influence of thermal spin waves and their interaction with the free spin waves is another

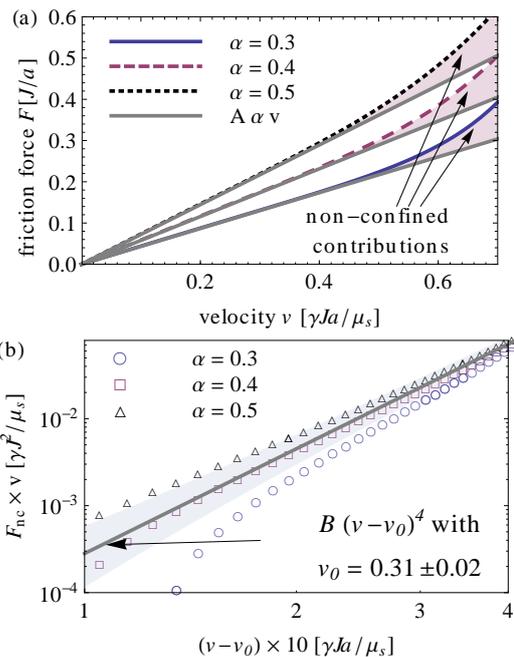


Fig. 6: (a) Friction force for several velocities, with the non-confined part marked by the shading. (b) Non-confined contributions to the friction force times velocity as well as the function $B(v - v_0)^4$, where v_0 has been taken from eq. (16).

open question. Studies dealing with this are already in progress and will be reported in a future work.

This work was supported by the German Research Foundation (DFG) via SFB 616 and the German Academic Exchange Service (DAAD) through the PROBRAL programme.

REFERENCES

- [1] URBACH M., KLAFTER J., GOURDON D. and ISRAELACHVILI J., *Nature*, **430** (2004) 525.
- [2] CORBERI F., GONNELLA G. and LAMURA A., *Phys. Rev. Lett.*, **81** (1998) 3852.
- [3] ACHARYYA M. and CHAKRABARTI B. K., *Phys. Rev. B*, **52** (1995) 6550.
- [4] KADAU D., HUCHT A. and WOLF D. E., *Phys. Rev. Lett.*, **101** (2008) 137205.
- [5] ANGST S., HUCHT A. and WOLF D. E., in preparation (2011).
- [6] HUCHT A., *Phys. Rev. E*, **80** (2009) 061138.
- [7] IGLÓI F., PLEIMLING M. and TURBAN L., *Phys. Rev. E*, **83** (2011) 041110.
- [8] HILHORST H. J., *J. Stat. Mech.*, **2011** (2011) P04009.
- [9] FUSCO C., WOLF D. E. and NOWAK U., *Phys. Rev. B*, **77** (2008) 174426.
- [10] MAGIERA M. P., BRENDL L., WOLF D. E. and NOWAK U., *Europhys. Lett.*, **87** (2009) 26002.

- [11] MAGIERA M. P., WOLF D. E., BRENDEL L. and NOWAK U., *IEEE Trans. Magn.*, **45** (2009) 3938.
- [12] MAGIERA M. P. and WOLF D. E., *Simulation of magnetic friction* in *Proc. of the NIC Symp. 2010*, edited by MÜNSTER G., WOLF D. E. and KREMER M., Vol. 3 of *IAS Series* (Forschungszentrum Jülich GmbH, Jülich, Germany) 2010 p. 243.
<http://hdl.handle.net/2128/3697>
- [13] DÉMERY V. and DEAN D. S., *Phys. Rev. Lett.*, **104** (2010) 080601.
- [14] LANDAU L. D. and LIFSHITZ E. M., *Phys. Z. Sowj.*, **8** (1935) 153.
- [15] GILBERT T. L., *IEEE Trans. Magn.*, **40** (2004) 3443.
- [16] NEUSSER S. and GRUNDLER D., *Adv. Mater.*, **21** (2009) 2927 .
- [17] SERGA A. A., CHUMAK A. V. and HILLEBRANDS B., *J. Phys. D-Appl. Phys.*, **43** (2010) 264002.
- [18] COEY J. M. D., *Magnetism and Magnetic Materials* (Cambridge University Press) 2010.